

From acene to graphene spectrum of π electrons with the use of the Green's function

Lyuba Malysheva and Alexander Onipko*

Bogolyubov Institute for Theoretical Physics, 03680 Kiev, Ukraine

Received 1 May 2008, accepted 16 May 2008

Published online 3 September 2008

PACS 31.15.ae, 61.46.–w, 73.22.–f, 73.63.–b

* Corresponding author: e-mail: aleon@ifm.liu.se, Phone: +46-13-288904, Fax: +46-13-28 8969

The origin of the spectrum of π electrons that results from the coupling of N \mathcal{N} -long acenes via C-C covalent bonding has been traced with the use of the Green function formalism.

Exact expressions of acene and graphene Green's functions, which are useful for analysis of the electronic properties of these macromolecules, are obtained and advanced to a form suitable for instructive applications.

© 2008 WILEY-VCH Verlag GmbH & Co. KGaA, Weinheim

1 Introduction Free standing graphene, a monoatomic layer of graphite, is a new material [1,2] that exhibits exceptional electronic quality [1–5] and a unique nature of charge carriers. On the one hand, electrons and holes appear as quasi-particles in condensed-matter physics when the Schrödinger equation governs our prediction of their behavior [6–16]. On the other hand, they behave as relativistic particles which are subject to the Dirac equation [17–22]. Much theoretical effort has been focused primarily on the electronic states of infinite graphene. In the continuum approximation, these states can be mapped into a Hamiltonian of 2+1 dimensional quantum electrodynamics with Dirac fermions. This description is based on the cone-like spectrum near the neutrality (zero-energy) points of the 2D graphite band structure, see [22] and references therein. Less attention has been paid to graphene as a molecular species. From this point of view, graphene can be considered as a macromolecule obtained by C-C bonding of acene chains as shown in Fig. 1. In certain aspects, the macromolecule model provides a better approximation for the description of real graphene structures [16], particularly, in the nanometer scale, where the continuous approximation is of limited value [23].

As is clear from Fig. 1, \mathcal{N} -long linear acenes are basic units of the $N \times \mathcal{N}$ sheet of the graphene honeycomb lattice, whereas \mathcal{N} -long cyclacenes play the same role for zigzag $(\mathcal{N},0)$ carbon nanotubes (CNTs). In this sense, the graphene and acene spectra are intimately interrelated. The

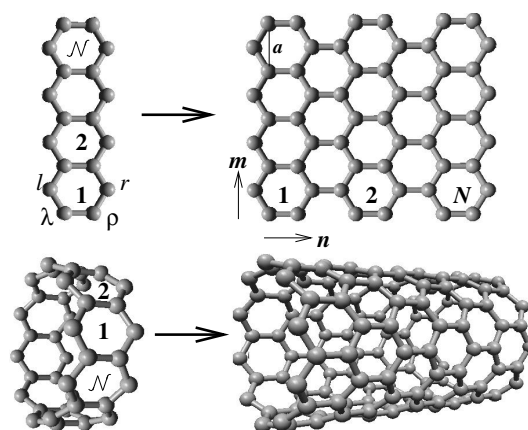


Figure 1 \mathcal{N} -long linear acene as a basic unit of the $N \times \mathcal{N}$ sheet of the graphene honeycomb lattice (up) and \mathcal{N} -long cyclacene playing the same role for zigzag $(\mathcal{N},0)$ carbon nanotubes (CNTs).

electronic structure of acenes, the semi-empirical description of which goes back to the Pariser and Parr classic works [24,25], is understood fairly well [26–28]. This study elucidates the relationship between the graphene and acene spectra. Keeping in mind subsequent applications, our analysis has been performed with the use of the Green's function method. All derivations are based on the

standard operator equation

$$G^M = [EI - H^M]^{-1}, \quad (1)$$

where H^M is the tight-binding Hamiltonian operator of acene ($M=A$) or graphene ($M=G$); the electron energy E is in units of $|t|$, t denotes the C-C hopping integral. For the Green's function matrix elements, notations $\langle m\alpha | G^A | m'\beta \rangle \equiv G_{m\alpha, m'\beta}^A$ and $\langle mn\alpha | G^G | m'n'\beta \rangle \equiv G_{mn\alpha, m'n'\beta}^G$ will be used for acene and graphene, respectively; $|m\alpha\rangle$ and $|mn\alpha\rangle$ denote $2p_z$ orbitals at the α th carbon atom of the m -th and mn -th hexagon, respectively, as shown in Fig. 1. The formal description of acenes and cyclacenes, and graphene and CNT is very similar. However, in the interests of simplicity, only the acene-graphene pair will be in focus. An extended discussion that also includes cyclacenes and zigzag CNTs can be found in Ref. [29]

2 Acene Green's function For linear acenes, the matrix form of solution to Eq. (1) is given by [30]

$$G_{m\alpha, m'\beta}^A = \frac{2}{\mathcal{N} + 1} \sum_{j=1}^{\mathcal{N}} g_{\alpha, \beta}^j \sin(\xi_j m) \sin(\xi_j m'), \quad (2)$$

where $\xi_j = \pi j / (\mathcal{N} + 1)$, $j = 1, 2, \dots, \mathcal{N}$, and

$$\mathcal{D}_j g_{\alpha, \beta}^j = \begin{cases} E [E^2 - 4 \cos^2(\xi_j/2) - 1], & \alpha = \beta = l, r, \\ 4 \cos^2(\xi_j/2), & \alpha = l(r), \beta = r(l), \end{cases} \quad (3)$$

where $\mathcal{D}_j = [E^2 - 4 \cos^2(\xi_j/2)]^2 - E^2$. For the rest of matrix elements, we obtain

$$G_{m\lambda, m'\{\rho\}}^A = \frac{\delta_{m, m'} \{ \frac{E}{1} \}}{E^2 - 1} + \frac{8}{\mathcal{N} + 1} \times \sum_{j=1}^{\mathcal{N}} g_{\alpha, \beta}^j \cos^2(\xi_j/2) \sin[\xi_j(m-1/2)] \sin[\xi_j(m'-1/2)], \quad (4)$$

$$\begin{aligned} & \mathcal{D}_j (E^2 - 1) g_{\alpha, \beta}^j \\ &= \begin{cases} E [E^2 - 4 \cos^2(\xi_j/2) + 1], & \alpha = \beta = \lambda, \rho, \\ 2E^2 - 4 \cos^2(\xi_j/2), & \alpha = \lambda(\rho), \beta = \rho(\lambda), \end{cases} \end{aligned} \quad (5)$$

and

$$G_{m\alpha, m'\beta}^A = \frac{4}{\mathcal{N} + 1} \sum_{j=1}^{\mathcal{N}} g_{\alpha, \beta}^j \cos(\xi_j/2) \sin[\xi_j(m-1/2)] \sin(\xi_j m'), \quad (6)$$

$$\mathcal{D}_j g_{\alpha, \beta}^j = \begin{cases} E^2 - 4 \cos^2(\xi_j/2), & \alpha = \lambda(\rho), \beta = l(r), \\ E, & \alpha = \lambda(\rho), \beta = r(l). \end{cases} \quad (7)$$

As shown in [16], the quantities $g_{l, l}^j = g_{r, r}^j$ and $g_{l, r}^j = g_{r, l}^j$ defined in Eq. (3) determine the dispersion relation for an $\mathcal{N} \times \mathcal{N}$ sheet of graphene $E(\kappa_j, \xi_j)$ via the equation

$$2g_{l, r}^j \cos \kappa_j = 1 - (g_{l, l}^j)^2 + (g_{l, r}^j)^2, \quad (8)$$

where κ_j is the second, complementing ξ_j quantum number. $2\mathcal{N}$ values of $\kappa_{j, \nu}^{\pm}$, $\nu = 0, 1, \dots, \mathcal{N} - 1$, for each j classify the graphene spectrum into $4\mathcal{N}\mathcal{N}$ j, ν levels; see below.

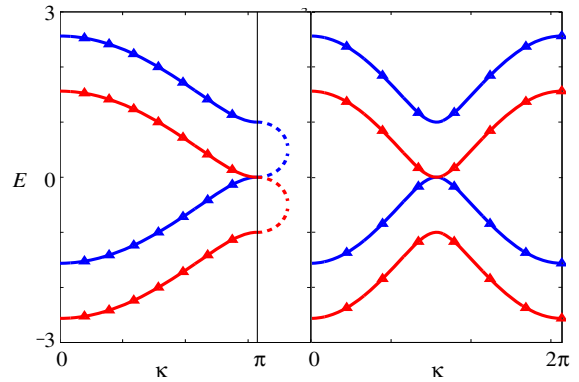


Figure 2 Band structure of polyacene, $E(\kappa=k^+)$ (red) and $E(\kappa=k^-)$ (blue), calculated from Eq. (9) for infinite linear acene (left panel) and cyclacene (right panel). Continuation to imaginary values of wave vectors, $k^{\pm} \rightarrow \pm \pi \pm i\delta$, $0 \leq \delta \leq 2 \ln((1 + \sqrt{17})/4) \approx 0.5$, is shown by dashed lines. Solid lines of the right panel for $\kappa \leq \pi$ repeat similar calculations of Ref. [27]. Triangles show energy levels for $\mathcal{N}=7$ according to Eq. (11).

By performing summation over j , it is possible to express the energy dependence of the acene Green's function in terms of (dimensionless) wave vectors k^+ and k^- , subjected to the equation

$$4 \cos^2(k^{\pm}/2) = E(E \pm 1). \quad (9)$$

For example, $G_{1\lambda(\rho), (\mathcal{N}+1)\lambda(\rho)}^A = G_{k^+} + G_{k^-}$, where

$$G_{k^{\pm}} = \frac{1}{2(E \pm 1)} \frac{\sin k^{\pm}}{\sin(\mathcal{N} + 1)k^{\pm}}. \quad (10)$$

Other matrix elements have similar expressions. As seen from Fig. 2, for the given energy, either both k^+ and k^- are real, or one is real, whereas the other one is imaginary. In the latter case, matrix elements which refer to opposite sites of the chain have two typical terms: One is exponential, $\sim \exp(-\sqrt{|E|}\mathcal{N})$, and the second term has a singular character. Hence, the probability of electron transmission through acenes ($\sim G_{1, (\mathcal{N}+1)}^A$) [31] can occur via partly coherent and partly tunneling mechanisms.

Tunneling governed by a single exponential factor, as it takes place in conjugated oligomers [31,32], is not possible. This is a reflection of the metallic nature of polyacenes [26,27].

2.1 Acene electron spectrum The acene electronic structure is determined by the equation $(E^2 - 1)\mathcal{D}_j = 0$; zeros of \mathcal{D}_j give a four-band spectrum

$$E_{c(v)}^{\pm} = +(-)\frac{1}{2} \left[\mp 1 \pm \sqrt{1 + 16 \cos^2(\xi_j/2)} \right], \quad (11)$$

where each of two conduction (*c*) and two valence (*v*) bands has \mathcal{N} levels. Note that two extra levels $E = \pm 1$ do not appear in Eq. (2) as poles of the acene Green's function. The states with these energies correspond to zero wave function amplitudes at *l* and *r* sites and thus, break the acene chain into λ - ρ "isolated" pairs.

For long chains $\mathcal{N} \gg 1$ and $|E| \ll 1$, spectrum (11) is well approximated by $E = \pm q_{\mu}^2$ with $q_{\mu} = \pi\mu/\mathcal{N}$, $\mu = 1, 2, \dots$. In the limit $\mathcal{N} \rightarrow \infty$, the quantum number ξ_j can be considered as a continuous variable, $\xi_j \rightarrow k$, and $q_{\mu} \rightarrow q = \pi - k$ acquires the meaning of *k* separation from the zero-energy point at $k = \pi$. The spectrum of polyacene (an infinite acene chain) that comes out from the spectra of linear acene and cyclacene, is shown in Fig. 2.

3 Graphene Green's function Similarly to Eq. (2), the matrix elements of the graphene Green's function can be represented in the form of an expansion

$$G_{mna, m'n'\beta}^G = \frac{2}{\mathcal{N} + 1} \sum_{j=1}^{\mathcal{N}} G_{na, n'\beta}^j \sin(\xi_j m) \sin(\xi_j m'), \quad (12)$$

where $G_{na, n'\beta}^j = G_{na, n'\beta}^{j+} + G_{na, n'\beta}^{j-}$. Here, we restrict ourselves to representative examples of matrix elements referring to the *l* and *r* sites, namely,

$$G_{1l, \{ \frac{1}{\mathcal{N}} \} \{ \frac{l}{r} \}}^{j\pm} = \frac{\begin{Bmatrix} g_{l,l}^j \sin(\kappa_j^{\pm} N) \\ g_{l,r}^j \sin \kappa_j^{\pm} \end{Bmatrix}}{\sin(\kappa_j^{\pm} N) - g_{l,r}^j \sin[\kappa_j^{\pm} (N - 1)]}, \quad (13)$$

where labels + and - correspond to, respectively, "plus" and "minus" branches of dispersion relation (8). This relation can be rewritten as [16]

$$E_{c(v)}^{j\pm} = +(-)\sqrt{1 + 4 \cos^2(\xi_j/2) \pm 4 |\cos(\xi_j/2) \cos(\kappa_j/2)|}. \quad (14)$$

Thus, quantum numbers $\kappa_{j\nu}^{\pm}$ are determined by poles of $G_{na, n'\beta}^{j\pm}$ as a function of κ_j^{\pm} , i.e., by the roots of the equation $\sin \kappa_j^{\pm} N - g_{l,r}^j \sin \kappa_j^{\pm} (N - 1) = 0$, or [16]

$$\sin \kappa_j^{\pm} N = \mp 2 \cos(\xi_j/2) \sin \kappa_j^{\pm} (N + 1/2), \quad (15)$$

which together with Eq. (14) gives energies of $4\mathcal{N}\mathcal{N} j, \nu$ levels. Additionally, the graphene spectrum contains two N -fold degenerate levels with $E = \pm 1$.

In most cases, it is an interval near the Fermi energy, where interesting physics occurs. Whithin this interval and for $N, \mathcal{N} \gg 1$, we have [33]

$$E_c^{(j^* \pm \mu)-} = \begin{cases} \sqrt{\mu^2 \Delta_G^2 + \kappa^2/4}, \\ \sqrt{(\mu \mp \frac{1}{3})^2 \Delta_G^2 + \kappa^2/4}, \end{cases} \quad (16)$$

where $\Delta_G = \sqrt{3}\pi/[2(\mathcal{N}+1)]$, $\mu \ll \mathcal{N}$, and the upper and lower lines refer to an integer and rational value of $2(\mathcal{N}+1)/3$, respectively. In the case of integer values of $2(\mathcal{N}+1)/3 = j^*$, say, for $\mathcal{N} = \mathcal{N}^*$, infinitely long armchair graphene ribbons (GRs) have a metallic spectrum. In contrast, for $\mathcal{N} = \mathcal{N}^* \pm 1$, the lowest energy mode is $j^* = 2(\mathcal{N}^* \pm 1)/3$, and the spectrum has a band gap ($E_g = 2\Delta_G/3$), as defined by the lower line in Eq. (16).

The Green's functions of graphene strips with the length N and $\mathcal{N} = \mathcal{N}^*$, $\mathcal{N}^* + 1$ and $\mathcal{N}^* - 1$ have a pronouncedly different appearance; see Fig. 3. In what follows, we concentrate on energy intervals below (above) the bottom (top) of the second lowest band of metallic GRs, $|E| \leq \Delta_G$, and within the band gap of semiconducting GRs, $|E| \leq E_g/2$. For these energies, the Green's functions shown in the mid and right panel in Fig. 3 are accurately reproduced by a single member of expansion (12), namely, by the j^* -th term. To reproduce the energy dependence of the Green's function illustrated in the left panel, two terms are needed, partial Green's functions j^* and $j^* + 1$.

As immediately follows from Eq. (16), the E - κ relation can be satisfied only by real and only by imaginary ($\kappa = i\delta$) values of the wave vector for metallic and semiconducting GRs, respectively. As a result, an exponential factor

$$G_{1l, Nr}^{j^*} \sim \exp\left(-2N\sqrt{(E_g/2)^2 - E^2}\right), \quad (17)$$

appears in the Green's function of semiconducting GRs. This factor governs the probability of single-mode electron/hole transmission through a potential barrier; see Ref. [34] of this issue.

For metallic GRs, the number of poles depends on N as, approximately, $[\sqrt{3}N/(\mathcal{N}+1) + 1/2]$. For semiconducting GRs with $\mathcal{N} = \mathcal{N}^* - 1$, there are no poles at all, but in the case of $\mathcal{N} = \mathcal{N}^* + 1$, there is a single pole under the condition $N > 0.9\sqrt{3}(\mathcal{N}+1)\pi - 1/2$ or, approximately $N > \mathcal{N}/2$. These peculiarities are illustrated in Fig. 3.

To conclude this report, the spectra and Green's functions of graphene and its building blocks, acenes have been discussed in parallel that provides a deeper insight into the origin and particularities of the graphene electronic structure. An exact analytical expression of the graphene Green's function is found in terms of an expansion over partial Green's functions. The character of the Green's

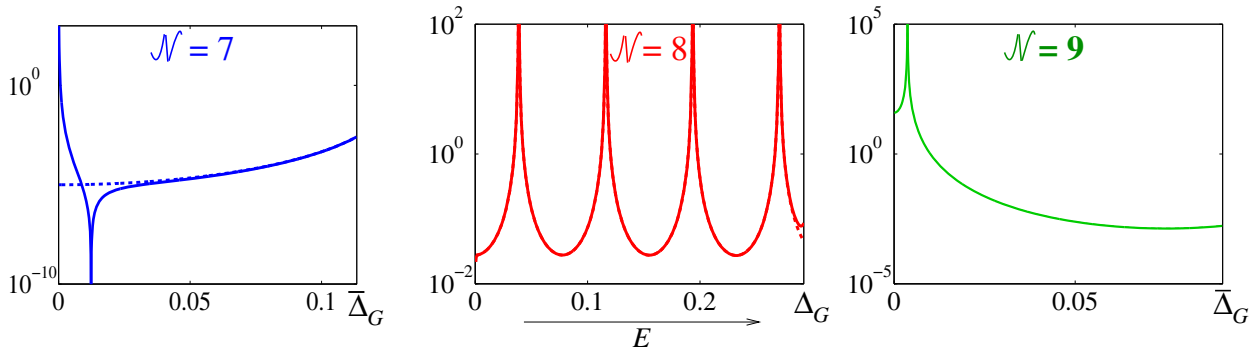


Figure 3 Green's function matrix element squared, $G_{11l,1Nr}^{G^2}$, $N=20$, for semiconducting (blue, green) and metallic (red) graphene strips; the correspondence between colors and \mathcal{N} values is the same, as in Fig. 4. An increase/decrease of N results in a shift of the deep and peak in the left and right panels, respectively, towards smaller/larger energies and also, in a larger/smaller number of peaks in the mid panel. Differences between the exact Green's function expansion and its approximation by the j^* -th term (mid and right panels), and by a sum of the j^* -th and (j^*+1) -th terms of the expansion (left panel) are vanishingly small. The dashed blue line shows an approximation by the j^* term. Notations $\bar{\Delta}_G = \Delta_G/3 = E_g/2 = \pi/[2\sqrt{3}(\mathcal{N}+1)]$ are explained in the text.

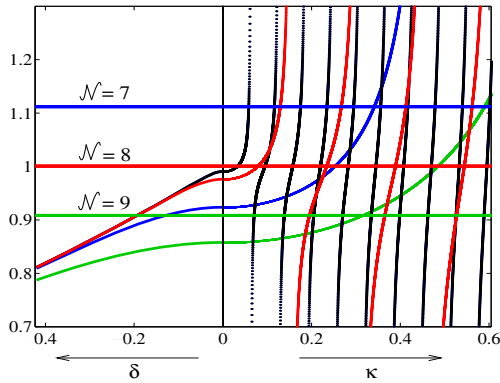


Figure 4 Solutions to Eq. (15), shown by intersections of black, red, and blue curves, corresponding to $N=50, 20$, and 6 , respectively, with three horizontal lines $2 \cos \xi_{j^*}/2$ for $\mathcal{N} = \mathcal{N}^*$ (red), \mathcal{N}^*-1 (blue), and \mathcal{N}^*+1 (green); $\mathcal{N}^*=8$. Green curve, representing $N=3$ ($< \mathcal{N}^*/2$) does not have intersections in the region of imaginary $\kappa = i\delta$; see text.

function singularities near the Fermi energy has been examined and shown to be qualitatively different for metallic and semiconducting graphene ribbons.

Acknowledgements This work was partly supported by Visby program of the Swedish Institute (SI).

References

[1] K. S. Novoselov, A. K. Geim, S. V. Morozov, D. Jiang, Y. Zhang, S. V. Dubonos, I. V. Grigorieva, and A. A. Firsov, *Science* **306**, 366 (2004).
 [2] K. S. Novoselov, D. Jiang, T. Booth, V. V. Khotkevich, S. V. Morozov, and A. K. Geim, *Proc. Nat. Acad. Sci.* **102**, 10451 (2005).

[3] K. S. Novoselov, A. K. Geim, S. V. Morozov, D. Jiang, M. I. Katsnelson, I. V. Grigorieva, S. V. Dubonos, and A. A. Firsov, *Nature (London)* **438**, 197 (2005).
 [4] Y. Zhang, Y.-W. Tan, H. L. Stormer, and P. Kim, *Nature (London)* **438**, 201 (2005).
 [5] A. K. Geim and K. S. Novoselov, *Nature Mater.* **6**, 183 (2007).
 [6] P. R. Wallace, *Phys. Rev. B* **9**, 622 (1947).
 [7] M. Fujita, K. Wakabayashi, K. Nakada, and K. Kusakabe, *J. Phys. Soc. Jpn.* **65**, 1920 (1996).
 [8] K. Nakada, M. Fujita, G. Dresselhaus, and M. S. Dresselhaus, *Phys. Rev. B* **54**, 17954 (1996).
 [9] R. Saito, G. Dresselhaus, and M. S. Dresselhaus, *Physical Properties of Carbon Nanotubes* (Imperial College, London, 1998).
 [10] K. Wakabayashi, M. Fujita, H. Ajiki, and M. Sigrüst, *Phys. Rev. B* **59**, 8271 (1999).
 [11] K. Wakabayashi, *Phys. Rev. B* **64**, 125428 (2001).
 [12] S. Reich, C. Thomsen, and J. Maultzsch, *Carbon Nanotubes: Basic concepts and Physical Properties* (Wiley-VCH, Weinheim, 2004).
 [13] N. M. R. Peres, A. H. Castro Neto, and F. Guinea, *Phys. Rev. B* **73**, 195411 (2006).
 [14] M. Kohmoto and Y. Hasegawa, *Phys. Rev. B* **76**, 205402 (2007).
 [15] K. Wakabayashi, Y. Takane, and M. Sigrüst, *Phys. Rev. Lett.* **99**, 036601 (2007).
 [16] L. Malysheva and A. Onipko, *Phys. Rev. Lett.* **100**, 186806 (2008).
 [17] G. W. Semenoff, *Phys. Rev. Lett.* **53**, 2449 (1984).
 [18] D. V. Khveshchenko, *Phys. Rev. Lett.* **87**, 206401 (2001).
 [19] T. Ando, *J. Phys. Soc. Japan* **74**, 777 (2002).
 [20] L. Brey and H. A. Fertig, *Phys. Rev. B* **73**, 235411 (2006).
 [21] Y. P. Gusynin, S. G. Sharapov, and J. P. Carbotte, *Phys. Rev. Lett.* **98**, 157402 (2007).
 [22] Y. P. Gusynin, S. G. Sharapov, and J. P. Carbotte, *Int. J. Mod. Phys. B* **21**, 4611 (2007).
 [23] L. Malysheva and A. Onipko, arXiv:0802.1522v1 [cond-mat.mes-hall].

- [24] R. Pariser and R. G. Parr, *J. Chem. Phys.* **21**, 466 (1953).
- [25] R. Pariser, *J. Chem. Phys.* **24**, 250 (1956).
- [26] M. Kertesz and R. Hoffmann, *Solid State Commun.* **47**, 97 (1983).
- [27] S. Kivelson and O.L. Chapman, *Phys. Rev. B* **28**, 7236 (1983).
- [28] K. N. Houk, P.S. Lee, and M. Nendel, *J. Org. Chem.* **66**, 5517 (2001).
- [29] L. Malysheva and A. Onipko, arXiv:0804.4552v1 [cond-mat.mes-hall].
- [30] Yu. Klymenko, unpublished.
- [31] A. Onipko and L. Malysheva, in: *Nano and Molecular Electronics Handbook*, edited by S.E. Lyshevski, Nano- and Microscience, Engineering, Technology, and Medicine Series (CRC Press, Taylor & Francis Group, Boca Raton, FL, 2007), chap. 23.
- [32] M. Magoga and C. Joachim, *Phys. Rev. B* **56**, 4722 (1997).
- [33] L. Malysheva and A. Onipko, *JETP Lett.*, No. 12 (2008), to be published; arXiv:0803.1761v1 [cond-mat.mes-hall].
- [34] Yu. Klymenko, O. Shevtsov, and A. Onipko, *phys. stat. sol. (b)* **245**, No. 10 (2008), this issue.